Intraoperative image correction using a biomechanical model of the human head with different material properties

A. Hagemann[1], K. Rohr[1], H. S. Stiehl[1], U. Spetzger[2], J. M. Gilsbach[2]

[1]Universität Hamburg, FB Informatik, AB Kognitive Systeme,
Vogt-Kölln-Straße 30, D-22527 Hamburg
Tel.: +49 (40) 42883 2577 Fax: +49 (40) 42883 2572
E-Mail: hagemann@informatik.uni-hamburg.de
[2]Neurochirurgische Klinik, Universitätsklinik der
Rheinisch-Westfälischen Technischen Hochschule (RWTH),
Pauwelstraße 30, D-52057 Aachen

Abstract. In order to improve the accuracy of image-guided neurosurgery, different biomechanical models have been developed to correct preoperative images w.r.t. intraoperative changes like brain shift or tumor resection. For the simulation of deformations of anatomical structures with different material properties, all existing biomechanical models use either appropriate boundary conditions or spatially varying material parameter values while assuming the same physical model for all anatomical structures. In this contribution, we propose a new approach which allows to couple different physical models. In our case, we simulate rigid, elastic, and fluid structures by using the appropriate physical description for each material, namely the Navier equation and the Stokes equation. To solve the resulting differential equations, we derive a linear matrix system for each region by applying the finite element method. Thereafter, the linear matrix systems are linked to one common linear matrix system. Our approach has been tested using synthetic as well as tomographic images. It turns out that the integrated treatment of rigid, elastic, and fluid structures significantly improves the predicted deformation results in comparison to a pure linear elastic model.

Keywords: biomechanical model, inhomogeneous materials, coupled regions, FEM, intraoperative image correction

1 Introduction

The accuracy of image-guided neurosurgery generally suffers from intraoperative changes of the brain anatomy due to, e.g., tumor resection or brain shift [1]. To improve upon navigation accuracy, a variety of biomechanical models were developed [2–5] to predict brain deformations and thus to correct the preoperative images w.r.t. surgery induced effects. Additionally, some biomechanical models exist within the scope of preoperative planning for registration purposes [6–8] which can be used likewise to predict brain deformations.

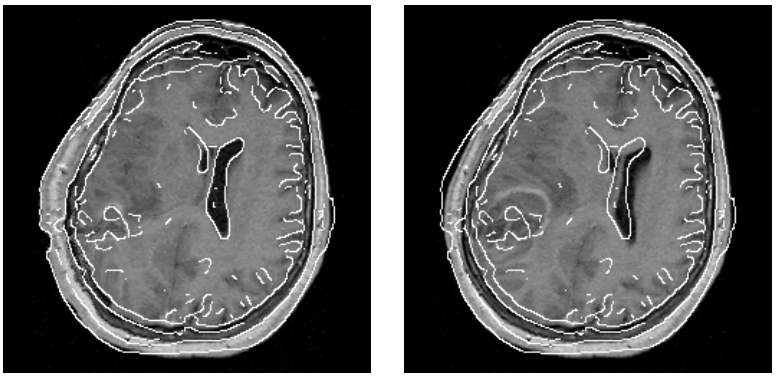

(a) (b)

Fig. 1. Simulation of fluids while treating them as rigid object: (a) registration result with overlaid edges of the original postoperative image while none of the correspondences were given within the vicinity of the ventricular system (dark elongated region in the middle of the image) and (b) while only two parallel correspondences were given directly at the ventricular system, leading to an unrealistic translation of the latter one.

All these models simulate different anatomical structures by either spatially varying the underlying material parameter values while assuming the same physical model for all anatomical structures [6, 2, 8, 5] or by applying appropriate boundary conditions [3, 4, 7]. An example for the latter case is the integration of the skull bone or the falx as a non-moving part (known as homogeneous *Dirichlet boundary condition*). However, this generally leads to a physically inadequate simulation, particularly in the case of combined elastic/fluid regions. For example, the ventricular system in [5] was modeled as a rigid object, which is motivated by the reported incompressibility of cerebrospinal fluid [9, 10]. Using this assumption, good registration results were obtained if none of the prescribed correspondences, which drive the deformation of the model, were given in the vicinity of the ventricular system. Otherwise the model gives a poor registration result, leading to an unrealistic deformation of the fluid region as shown in Figure 1. An approach that directly simulates the physical behaviour of fluids through the use of the *Navier-Stokes equation* is the model of Lester *et al.* [8], which is motivated by the homogeneous fluid model of Christensen [11]. But in both cases, it is assumed that all anatomical structures behave like fluids which is generally not the case.

In order to improve the simulation of head deformations, we extend our biomechanical model [5] such that it allows to cope with anatomical structures consisting of *rigid*, *elastic*, and *fluid* materials while using the appropriate physical descriptions, namely the *Navier equation* and the *Stokes equation*. Our approach is based on the well-established physical theory of continuum mechanics to handle inhomogeneous materials. With this scheme, an inhomogeneous domain is

divided into homogeneous regions, each simulating a different material by using an appropriate material description. To discretize the problem, we apply the *finite element method* (FEM) to each region, resulting in a set of sparse linear matrix systems. These matrix systems can be assembled together into a single common matrix system via appropriate boundary conditions, which establish a physical link between the corresponding regions. Instead of using external forces, which are hard or even impossible to derive from corresponding images, we use a set of given correspondences to drive the deformation of the image. In our approach, it is ensured that the prescribed correspondences are exactly fulfilled. Experiments with synthetic as well as real tomographic images have been carried out and the results are compared against our previous model to assess the physical plausibility of the predicted deformations.

2 Approach

Motivated by the physical properties of cerebrospinal fluid [9, 10], we use the Stokes equation as physical description for *incompressible* fluids:

$$-\nabla p + \mu^\star \nabla^2 \mathbf{v} + \mathbf{f} = \mathbf{0}. \tag{1}$$

This is in contrast to [11, 8], where the Navier-Stokes equation has been used to simulate *compressible* fluids, and to [3] where the fluid region is allowed to deform almost freely. The elastic and rigid materials are modeled by the Navier equation

$$(\lambda + \mu)\nabla \mathrm{div}[\mathbf{u}] + \mu \nabla^2 \mathbf{u} + \mathbf{f} = \mathbf{0}, \tag{2}$$

and it is furthermore assumed that *Cauchy's formula*

$$\boldsymbol{\sigma}\mathbf{n} = \mathbf{g} \tag{3}$$

holds on all boundaries. Here, ∇ denotes the common Nabla operator, p the unknown pressure, $\mu^\star$ the viscosity parameter, $\mathbf{v}$ the unknown velocity field, $\mathbf{f}$ the applied body forces, λ and μ the *Lamé constants*, $\mathbf{u}$ the unknown displacement field, $\boldsymbol{\sigma}$ the *Eulerian stress tensor*, $\mathbf{n}$ the unit vector normal to the surface considered, and $\mathbf{g}$ the forces acting on this surface. Applying the finite element method to (1) and (2) and substitution of (3) yields in both cases a linear equation system

$$\mathbf{A}\mathbf{x} = \mathbf{f} + \mathbf{g}, \tag{4}$$

where $\mathbf{x}$ contains all unknown velocity and pressure coefficients or displacement coefficients, respectively. However, problems arise in determining the displacement field $\mathbf{u}$ for a fluid due to the common formulation of the Stokes equation in the *Eulerian configuration* to cope with large deformations. In contrast, the Navier equation is formulated in the *Lagrangian configuration* which ensures a proper definition of the boundaries. To solve this contradiction, we restrict the

deformation field to be infinitesimal, as implicitly done when using the Eulerian stress tensor and the Navier equation. This restriction allows an approximation of the displacements $\mathbf{u}$ by a multiplication of the velocities $\mathbf{v}$ with a small time interval dt, i.e. $\mathbf{u} = \mathbf{v}dt$ [12].

So far, each matrix system (4) contains the physical description of a *homogeneous* body only. The division of an *inhomogeneous* body Ω into a set of homogeneous regions Ω_i according to the underlying anatomical structures leads to an appropriate set of linear equation systems which can be physically linked by the *compatibility* and *equilibrium* boundary conditions [13, 12]: The former condition states, that the displacements $\mathbf{u}^\Gamma$ at the common boundary Γ between, e.g., two subregions Ω_i and Ω_j must be equal, while the latter one states that in the equilibrium case, the sum of all surface forces acting on Γ must be zero. The introduction of these boundary conditions, along with further assuming homogeneous body forces $\mathbf{f}$ over $\Omega = \Omega_i \cup \Omega_j$, allows a coupling of both linear systems:

$$\begin{pmatrix} \mathbf{A}_{11}^i & \mathbf{A}_{1\Gamma}^i & \mathbf{0} \\ \mathbf{A}_{\Gamma 1}^i & \mathbf{A}_{\Gamma\Gamma}^i + \mathbf{A}_{\Gamma\Gamma}^j & \mathbf{A}_{\Gamma 1}^j \\ \mathbf{0} & \mathbf{A}_{1\Gamma}^j & \mathbf{A}_{11}^j \end{pmatrix} \begin{pmatrix} \mathbf{u}^i \\ \mathbf{u}^\Gamma \\ \mathbf{u}^j \end{pmatrix} = \begin{pmatrix} \mathbf{f} + \mathbf{g}^i \\ \mathbf{f} \\ \mathbf{f} + \mathbf{g}^j \end{pmatrix}. \tag{5}$$

With $\mathbf{A}_{11}^i$ etc., we denote the submatrices of the corresponding stiffness matrices $\mathbf{A}^i$ and $\mathbf{A}^j$ for the subregions Ω_i and Ω_j, respectively. An index including Γ, as appearing in $\mathbf{A}_{1\Gamma}^i$ etc., indicates those submatrices which comprise finite elements belonging to the common boundary Γ between both regions. Based on (5) we are able to simulate the physical behaviour of an inhomogeneous body comprising rigid, elastic, and fluid parts.

In order to ensure the solvability of (5), we use for the fluid regions so-called $Q_2 - P_1$ *Crouzeix-Raviart* finite elements [14] with biquadratic polynomials for the velocity (resp. displacement) approximation and a linear, discontinuous approximation of the pressure, including two derivatives. At rigid and elastic regions, nine-node quadrilateral finite elements are applied. Nevertheless, problems arise with both types of elements due to the large number of associated degrees-of-freedom, which count to 21 resp. 18 per finite element in the 2D case. As a consequence of the resulting large linear equation system, only 2D images with a relatively small number of pixels can be handled so far.

To drive the deformation we apply homogeneous Dirichlet boundary conditions at the image borders and use given landmark correspondences instead of forces [5]. These correspondences can be easily integrated into the linear equation system, as described in Peckar *et al.* [15], and are always exactly satisfied by the resulting deformation.

3 Experiments

Our coupled rigid/elastic/fluid model has been tested for the cases of synthetic and tomographic images as shown in Figures 2(a) and (c). To assess the physical plausibility of our new model, we compared the results with those predicted

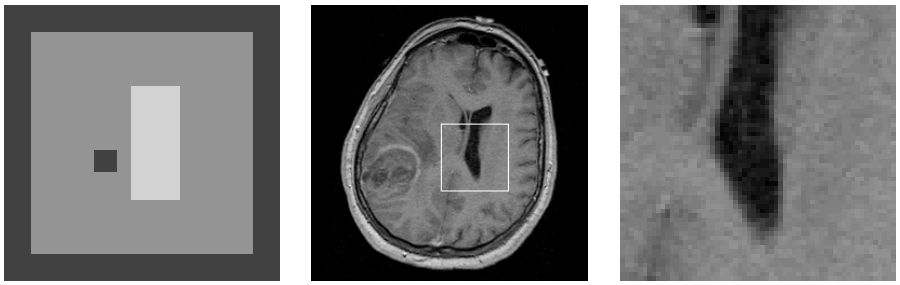

(a) (b) (c)

Fig. 2. Our synthetic image (a) comprises three different materials: rigid skull bone (black), cerebrospinal fluid (bright grey), and elastic brain tissue (dark grey). The used tomographic image (c) stems from a section of the ventricular system of the original preoperative image (b).

by our purely linear elastic model [5] in which we assumed at first a homogeneous elastic body and, at second, an inhomogeneous elastic body with elastic brain tissue, rigid skull bone, and fluid treated as a rigid object. As mentioned above, this kind of simulation was motivated by the reported incompressibility of cerebrospinal fluid. In the following, we refer to these three approaches as homogeneous elastic model, inhomogeneous elastic model, and inhomogeneous elastic/fluid model, respectively. As material parameter values we used the values determined in [5] for the Lamé constants and a heuristically chosen value of $0.01[Ns/m^2]$ for the viscosity parameter $\mu^\star$ due to the lack of other reported values.

In our first experiment, we simulated the movement of a squared, rigid object, which may represent an instrument for surgery, a foreign body, or a particle of skull bone, in the direction of a nearby fluid region, using the synthetic image shown in Figure 2(a). For simplicity, this movement is modeled as pure translation of the squared object using two parallel correspondences defined by $\mathbf{u} = (7.0, -4.0)^T$. We expect that the resulting deformation leads to a pure translation of the rigid object in the direction of the fluid region which should deform accordingly. As can be seen from the calculated results and corresponding grid deformations in Figures 3(a) and (d), the homogeneous elastic model results in a deformation where both, the object and the surrounding skull bone were deformed which is in contrast to rigid material behavior. With the inhomogeneous elastic model this is not the case, but the assumed rigidity of fluid leads to physically incorrect violations of the grid topology as depicted in Figures 3(b) and (e). Additionally, no deformation occurs in the fluid region and the soft material between the object and fluid regions is no longer visible (note, that the rigid and elastic parts after deformation lie one above the other). A completely different, physically adequate behavior shows our inhomogeneous elastic/fluid model. Here, the shape of the rigid object is still preserved while the complete

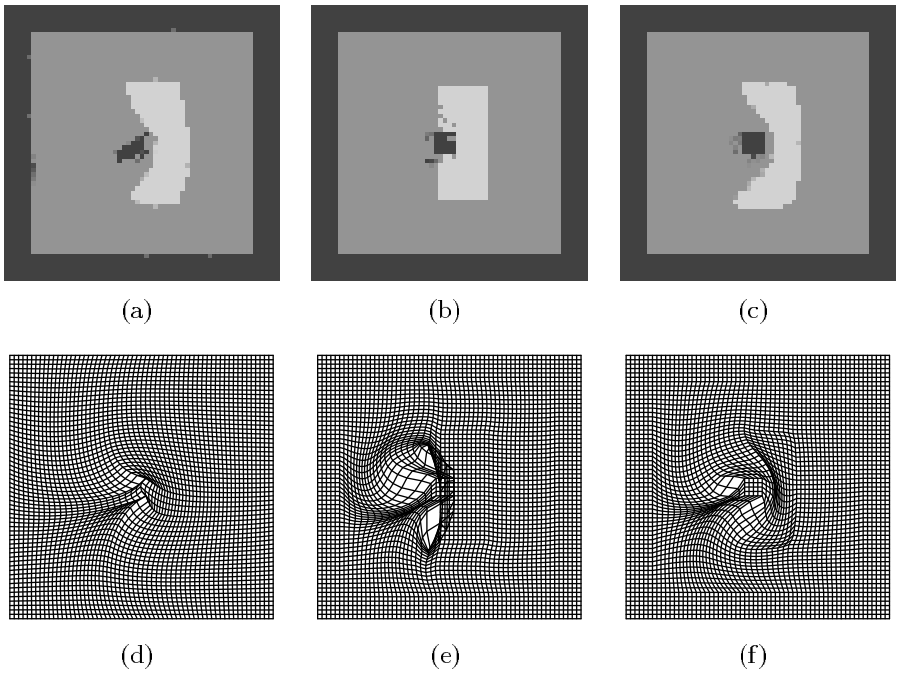

Fig. 3. Calculated images (top row) and corresponding grid deformations (bottom row) using (a) a homogeneous elastic model, (b) an inhomogeneous elastic model, and (c) an inhomogeneous elastic/fluid model.

deformation takes place in the fluid and brain tissue regions as shown in Figures 3(c) and (f).

For our second experiment with a real tomographic image, we used a section of the preoperative MR image shown in Figure 2(b). The resulting image of size 61×61 pixels shows a part of the ventricular system (which is a fluid region) surrounded by elastic brain tissue as depicted in Figure 2(c). In order to distinguish between both regions, we applied a Canny edge detector to the image. Thereafter, the resulting segmentation has been locally corrected to match with the underlying finite element mesh such that the resulting segmentation follows exactly the finite element boundaries.

Figure 4 shows the results and corresponding grid deformations for 8 parallel correspondences, defined as $\mathbf{u} = (7.0, 0.0)^T$, and prescribed at the left side of the ventricular system. Using the homogeneous elastic model, a remarkably bended shape of the ventricular system results, see Figure 4(a). As indicated by the grid deformation in Figure 4(d) and the displacement vector field shown in Figure 5(a), this bending is symmetric with regard to the applied correspondences. Significant displacements occur in a rather local neighbourhood, i.e. no displacements are propagated to remote parts of the image. In contrast, the inhomogeneous elastic model leads to a corrupted and physically incorrect result

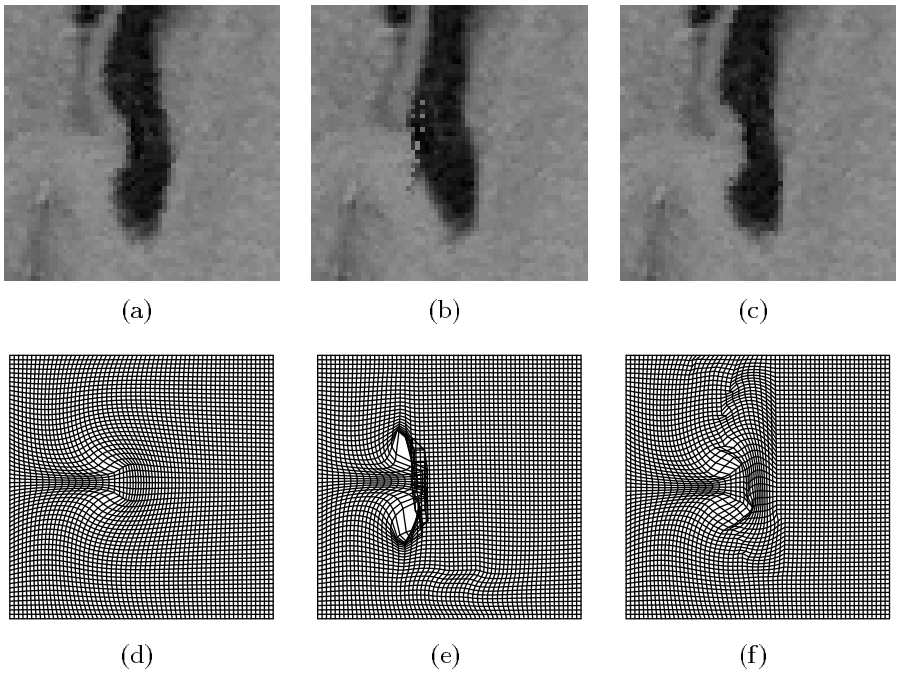

Fig. 4. Calculated images (top row) and corresponding grid deformations (bottom row) while using (a) the homogeneous elastic model, (b) the inhomogeneous elastic model, and (c) the inhomogeneous elastic/fluid model.

according to a violation of the underlying topology, which is clearly visible in the grid deformation shown in Figure 4(e) and the corresponding displacement vector field in Figure 5(b). Additionally, the shape of the ventricular system is nearly preserved thus indicating that the inhomogeneous elastic model is insufficient in this case.

Our inhomogeneous elastic/fluid model again results in a completely different, physically plausible behaviour, see Figures 4(c) and (f): According to the shape of the enclosed fluid region, the predicted deformation is non-symmetric with regard to the given correspondences. Also, the displacement vectors of the fluid region clearly spread out to remote parts of the region, i.e. material flows to the upper part of the image. The result is a roughly straight right border of the ventricular system. Interestingly, the pressure of the fluid onto the brain tissue at the right side is nearly uniformly distributed as indicated by the resulting overall small displacements of the brain tissue there, see Figure 5(c).

4 Summary

We proposed a new biomechanical model of the human head for image correction purposes based on the finite element method. The model uses the theory of

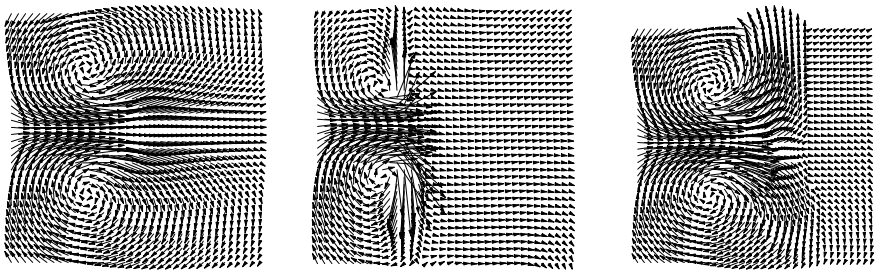

(a) (b) (c)

Fig. 5. Parts of the calculated displacement vector fields for (a) the homogeneous elastic model, (b) the inhomogeneous elastic model, and (c) the inhomogeneous elastic/fluid model, respectively. The sections were taken from the middle of the image.

continuum mechanics to simulate the physical deformation behavior of coupled rigid, elastic, and fluid regions. Experiments with synthetic as well as tomographic images have been carried out to assess the physical plausibility of the predicted deformation results. It turns out that our new approach leads to a significant improvement of the predicted results as compared to a pure linear elastic model. We expect that the incorporation of more advanced constitutive equations for brain tissue and other anatomical structures will further improve the results. Additional work will be carried out to reduce the size of the overall linear matrix system for the purpose of allowing to handle larger image sizes.

5 Acknowledgement

Support of Philips Research Laboratories Hamburg, project IMAGINE (IMage- and Atlas-Guided Interventions in NEurosurgery), is gratefully acknowledged.

References

1. D. L. G. Hill, C. R. Maurer, R. J. Maciunas, J. A. Barwise, J. M. Fitzpatrick, and M. Y. Wang. Measurement of Intraoperative Brain Surface Deformation under a Craniotomy. *Neurosurgery*, 43(3):514–526, September 1998.
2. R. D. Bucholz, D. D. Yeh, J. Trobaugh, L. L. McDurmont, C. Sturm, C. Baumann, J. M. Henderson, A. Levy, and P. Kessman. The Correction of Stereotactic Inaccuracy Caused by Brain Shift Using an Intraoperative Ultrasound Device. In J. Troccaz, E. Grimson, and R. Mösges, editors, *Computer Vision, Virtual Reality and Robotics in Medicine and Medical Robotics and Computer-Assisted Surgery (CVRMed-MRCAS'97)*, volume 1205 of *Lecture Notes in Computer Science*, pages 459–466, Grenoble, France, 1997. Springer Verlag.
3. P. J. Edwards, D. L. G. Hill, J. A. Little, and D. J. Hawkes. A three-component deformation model for image-guided surgery. *Medical Image Analysis*, 2(4):355–367, 1998.

4. O. Škrinjar, D. Spencer, and J. Duncan. Brain Shift Modeling for Use in Neurosurgery. In W. M. Wells, A. Colchester, and S. Delp, editors, *Medical Image Computing and Computer-Assisted Intervention (MICCAI'98)*, number 1496 in Lecture Notes in Computer Science, pages 641–648. Springer Verlag, October 1998.
5. A. Hagemann, K. Rohr, H. S. Stiehl, U. Spetzger, and J. M. Gilsbach. Nonrigid matching of tomographic images based on a biomechanical model of the human head. In K. Hanson, editor, *Medical Imaging 1999 – Image Processing (MI'99)*, Proceedings of the SPIE International Symposium, pages 583–592, San Diego, USA, February 1999.
6. C. Davatzikos. Nonlinear Registration of Brain Images Using Deformable Models. In M. E. Kavanaugh, editor, *Proceedings of the IEEE Workshop on Mathematical Methods in Biomedical Image Analysis*, pages 94–103, San Francisco, USA, June 1996.
7. S. K. Kyriacou and C. Davatzikos. A Biomechanical Model of Soft Tissue Deformation, with Applications to Non-rigid Registration of Brain Images with Tumor Pathology. In W. M. Wells, A. Colchester, and S. Delp, editors, *Medical Image Computing and Computer-Assisted Intervention (MICCAI'98)*, number 1496 in Lecture Notes in Computer Science, pages 531–538. Springer Verlag, October 1998.
8. H. Lester, S. R. Arridge, and K. M. Jansons. Local deformation metrics and nonlinear registration using a fluid model with variable viscosity. In E. Berry, D. Hogg, K. V. Mardia, and M. A. Smith, editors, *Proceedings of the Medical Image Understanding and Analysis (MIUA'98) Conference, Leeds, UK*, pages 44–48. University of Leeds, July 1998.
9. K. B. Sahay, R. Mehrotra, U. Sachdeva, and A. K. Banerji. Elastomechanical characterization of brain tissues. *Journal of Biomechanics*, 25(3):319–326, March 1992.
10. Y. Tada, T. Nagashima, and M. Takada. Biomechanics of brain tissue (simulation of cerebrospinal fluid flow). *JSME International Journal, Series A (Mechanics and Material Engineering)*, 37(2):188–194, April 1994.
11. G. E. Christensen, R. D. Rabbitt, and M. I. Miller. Deformable templates using large deformation kinematics. *IEEE Transactions on Image Processing*, 5(10):1435–1447, October 1996.
12. Y. C. Fung. *A First Course In Continuum Mechanics*. Prentice-Hall, 1994.
13. H. Kardestuncer and D. H. Norrie. *Finite Element Handbook*. McGraw-Hill Company, 1987.
14. C. Cuvelier, A. Segal, and A. A. van Steenhoven. *Finite Element Methods and Navier-Stokes Equations*. D. Reidel Publishing Company, 1986.
15. W. Peckar, C. Schnörr, K. Rohr, and H. S. Stiehl. Two-Step Parameter-Free Elastic Image Registration with Prescribed Point Displacements. *9th Int. Conf. on Image Analysis and Processing (ICIAP'97)*, 1310:527–534, 1997.